POLITECNICO DI TORINO
Repository ISTITUZIONALE

Effect of Progressive Integration of On-Board Systems Design Discipline in an MDA Framework for Aircraft Design with Different Level of Systems Electrification

(Article begins on next page)

18 October 2022

Effect of Progressive Integration of On-Board Systems Design Discipline in an MDA Framework for Aircraft Design with Different Level of Systems Electrification

Marco Fioriti [1],*, Pierluigi Della Vecchia [2] and Giuseppa Donelli [3]

[1] Politecnico di Torino, Department of Mechanical and Aerospace Engineering, 10100 Turin, Italy
[2] Department of Industrial Engineering, University of Naples Federico II, 80100 Naples, Italy;
    pierluigi.dellavecchia@unina.it
[3] German Aerospace Center (DLR), Institute of System Architectures in Aeronautics, 21129 Hamburg,
    Germany; giuseppa.donelli@dlr.de
* Correspondence: marco.fioriti@polito.it

Abstract: The on-board design discipline is sometimes ignored during the first aircraft design iterations. It might be understandable when a single on-board system architecture is considered, especially when a conventional architecture is selected. However, seeing the trend towards systems electrification, multiple architectures can be defined and each one should be evaluated during the first tradeoff studies. In this way, the systems design discipline should be integrated from the first design iterations. This paper deals with a progressive integration of the discipline to examine the partial or total effect of the systems design inside an MDA workflow. The study is carried out from a systems design perspective, analyzing the effect of electrification on aircraft design, with different MDA workflow arrangements. Starting from a non-iterative systems design, other disciplines such as aircraft performance, engine design, and aircraft synthesis are gradually added, increasing the sensibility of the aircraft design to the different systems architectures. The results show an error of 40% in on-board systems assessment when the discipline is not fully integrated. Finally, using the workflow which allows for greater integration, interesting differences can be noted when comparing systems with different levels of electrification. A possible mass saving of 2.6% of aircraft MTOM can be reached by properly selecting the systems technologies used.

Keywords: on-board system design; collaborative MDA; aircraft design

1. Introduction

In the last decades, aviation has been called to increase the safety, efficiency, and remunerability of its products. This led to a continuous aircraft refinement and optimization in different disciplinary areas. With the aim of further improving the present aeronautical products, innovative solutions have to be applied. In this context, one of the most promising solutions is aircraft electrification. This trend started some years ago, defining the More Electric Aircraft (MEA) and All Electric Aircraft (AEA) concepts, where the electrification of the aircraft subsystems is pursued. The trend towards on-board systems (OBS) electrification provides different benefits. Firstly, electrified OBS should reduce fuel consumption because of their greater efficiency [1–3]. This is particularly true when the electrification of the Environmental Control System (ECS) and Ice Protection System (IPS) are considered. Usually, the ECS and IPS are supplied by the engine compressors through the pneumatic system. In general, all the OBS options able to achieve bleedless engine technology (i.e., avoiding the use of compressed air from the engine compressors) produce beneficial effects on propulsion system efficiency. Secondly, electrified OBS are more maintainable, testable, and their status can be easily monitored, positively impacting the

operational cost [1,4–6]. This is achieved mainly by electrifying the Flight Control System (FCS) and Landing Gear System (LGS), avoiding the use of hydraulic technology. The hydraulic equipment is usually difficult to test and requires significant effort to be maintained. The MEA and AEA initiatives are providing several new OBS architectures with different levels of electrification. This greatly differs from a few decades ago when only one conventional (i.e., systems using hydraulic and bleed technologies) architecture was considered and the majority of preliminary design models included the OBS as a fixed percentage of the aircraft mass as the first design attempt [7–9]. Similarly, nearly all Multidisciplinary Design Analysis and Optimization (MDAO) studies, carried out for aircraft preliminary designs, do not involve the OBS discipline, focusing on aerodynamics, control, structure, and propulsion designs [10–12]. This may perhaps be acceptable when faced with conventional OBS architecture, assuming mass and volume values supported by statistic equations based on previous products. However, this approximation is not acceptable when MEA and AEA architectures are concerned. Each of these architectures deliver different effects at aircraft level in terms of mass, volume needed and power requirement, to only mention the main parameters affecting the aircraft design. Therefore, considering the electrification trend, the OBS design discipline should be fully included from the first aircraft design iterations, evolving together with the other disciplines to obtain an optimal product.

The integration of the OBS discipline in an MDAO workflow is currently under investigation by some researchers with different approaches [13–16]. All of them proposed the integration of OBS design, showing its advantages and complexities, but without comparing the results obtained using the proposed approach with the standard one (i.e., OBS design not integrated). Compared to other studies, the present paper deals with the progressive integration of the OBS design in a distributed MDAO workflow in order to analyze the mutual effects of OBS and aircraft design and to understand their actual contributions. In particular, the study permits the better evaluation of OBS architectures with different levels of electrification and, at the same time, an understanding of the most appropriate integration depth. In this way, three workflows are proposed, each one with a different integration depth. Four OBS architectures, with an increasing use of electrified systems, are studied by means of the three workflows. A small regional turboprop aircraft is defined as a reference. The electrification of this aircraft category is even more interesting since the trend towards propulsion system electrification.

The present work has been carried out in the frame of the AGILE4.0 (AGILE4.0 research project. Retrieved 14 March 2022 online: website: https://www.agile4.eu/) European research project [16] that has the objectives to reduce the time-to-market and the development cost of new products integrating new disciplines into traditional MDAO workflows.

The paper is divided in three main sections. In Section 3, the reference aircraft and the different OBS architectures are described, and the increasing electrification levels are identified. The three MDA workflows are described and discussed in Section 4. In Section 5, the results are reported, emphasizing the effect on the OBS assessment of adding and increasing the number of disciplines in the MDA/MDO workflow. Finally, the conclusions have been drawn also highlighting the next expected developments.

2. Reference Aircraft and OBS Architectures

To perform a quantitative analysis, a reference aircraft has been selected. Considering the interest towards the complete electrification of the small regional turboprop category, an aircraft carrying 19 passengers has been selected. The Top-Level Aircraft Requirements (TLARs), listed in Table 1, show a small transport aircraft able to connect small airports or a small airport with a hub, also at a large distance. The TLARs are mainly defined having the Beechcraft 1900D as a reference. The maximum take-off mass (MTOM) is limited to 8600 kg to comply with CS23 regulations [17].

Table 1. Reference aircraft TLARs.

N. of passengers	19
Maximum Range	1500 km
Speed	0.45 M @ 7620 m
Operative Ceiling	7620 m
TOFL	800 m
MTOM	≤8600 kg

Among the several possible OBS architectures that could be defined, four of the more promising have been considered for this kind of aircraft. Each of them has a different electrification level which has been defined starting from a different aim. The electrification level L_E is here defined as the ratio of the non-propulsive power produced by the electric system P_E and the total non-propulsive power P_T [18]:

$$L_E = \frac{P_E}{P_T} \tag{1}$$

The L_E is a parameter that assumes values always between 0 and 1.

The first architecture considered is the conventional one depicted in Figure 1a. It represents the standard OBS arrangement for a turboprop aircraft and it has the lowest value of L_E. Three different kinds of power are generated and distributed; they are electric, hydraulic, and pneumatic power. The Electrical Power Generation and Distribution System (EPGDS) consists of two redundant lanes. The electric power is generated by two 28 VDC starter generators (one per engine) and distributed by two PPDUs (Primary Power Distribution Units) that supply all the main electric utilities. Two inverters supply a double 115 VAC bus for some avionic equipment and some parts of the IPS by means of SPDUs (Secondary Power Distribution Units). The electric system supplies the fuel system, the avionics, the lights and furnishing, and part of the IPS (i.e., probes, sensors, propellers' leading edges). The Hydraulic Power Generation and Distribution System (HPGDS) comprises two lanes powered by two engine driven pumps (EDP) rated at 20.7 MPa. The HPGDS supplies the landing gear and the flap actuators. Finally, the pneumatic power is provided by the engine's bleed system rated at 5 bar. The pneumatic power is supplied to the ECS and part of the IPS. In particular, the pneumatic power is used by the wing and tail IPS to inflate and deflate the leading-edge boots. It is worth noting that the FCS (apart from the flap that is hydraulically driven) for this aircraft category relies on the pilots' force and the control surfaces are mechanically connected with the pilots' controls.

The first example of MEA architecture, called MEA1, is depicted in Figure 1b. Compared to the conventional architecture, the HPGDS is completely removed. The flap actuators are replaced by Electro Hydrostatic Actuators (EHA). In the same way, the actuators of the braking, steering and retracting systems of the landing gear are EHA. Usually, the EHA need to be supplied by a high voltage 270 VDC power bus. For this reason, and to reduce the mass of the electric system, the EPGDS of the MEA1 architecture consists of two 270 VDC busses and two 28 VDC busses. The high voltage busses supplied the greater part of the utility systems, whereas the avionic system is connected to the low voltage busses. Two high voltage starter generators power the EPGDS main busses, and two DC-DC converters provide power to the low voltage bus. No changes are made to the pneumatic system which still relies on the engine bleed system. Since the power required by the flap and landing gear is quite restrained and not continuous, the MEA1 architecture fairly increases the L_E. Its main advantage is to reduce the overall mass of the OBS by complete removal of the HPGDS.
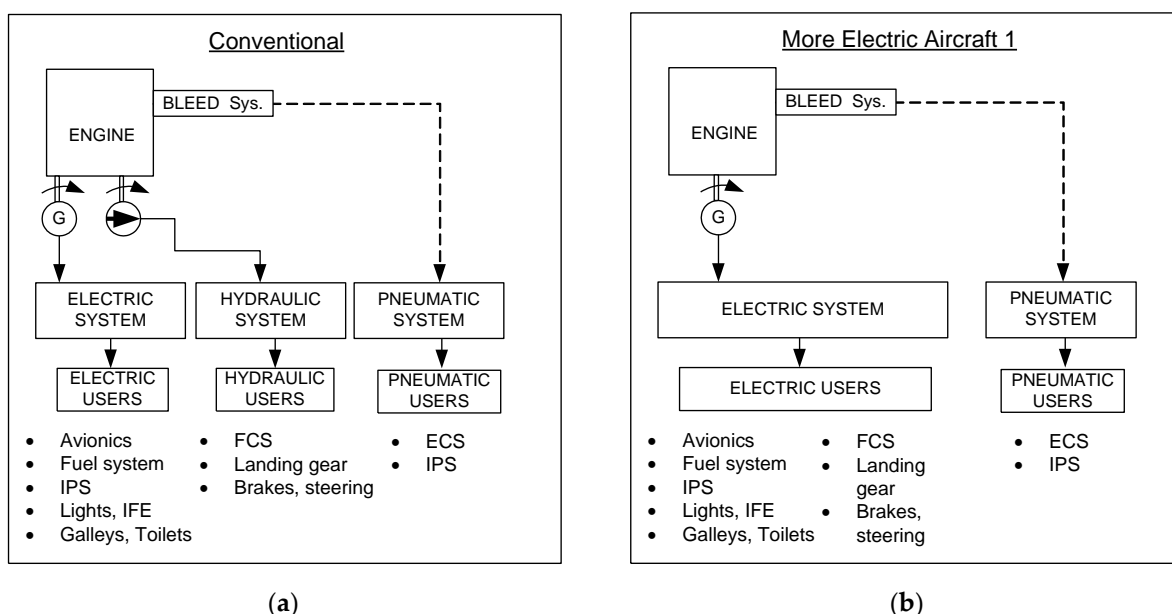
Figure 1. Conventional (**a**) and more electric n.1 (**b**) OBS architectures.

Conversely, the second MEA architecture (Figure 2a), here called MEA2, aims more at increasing the L_E, to optimize the power consumption, than achieving a mass saving. The main difference, compared to the conventional architecture, is the removal of the engine bleed system. The pneumatic power is generated by a series of centrifugal compressors arranged in two lanes for redundancy. The compressors are driven by electric motors connected to the EPGDS. Thus, the pneumatic power generation is completely electrified allowing for the bleedless technology.
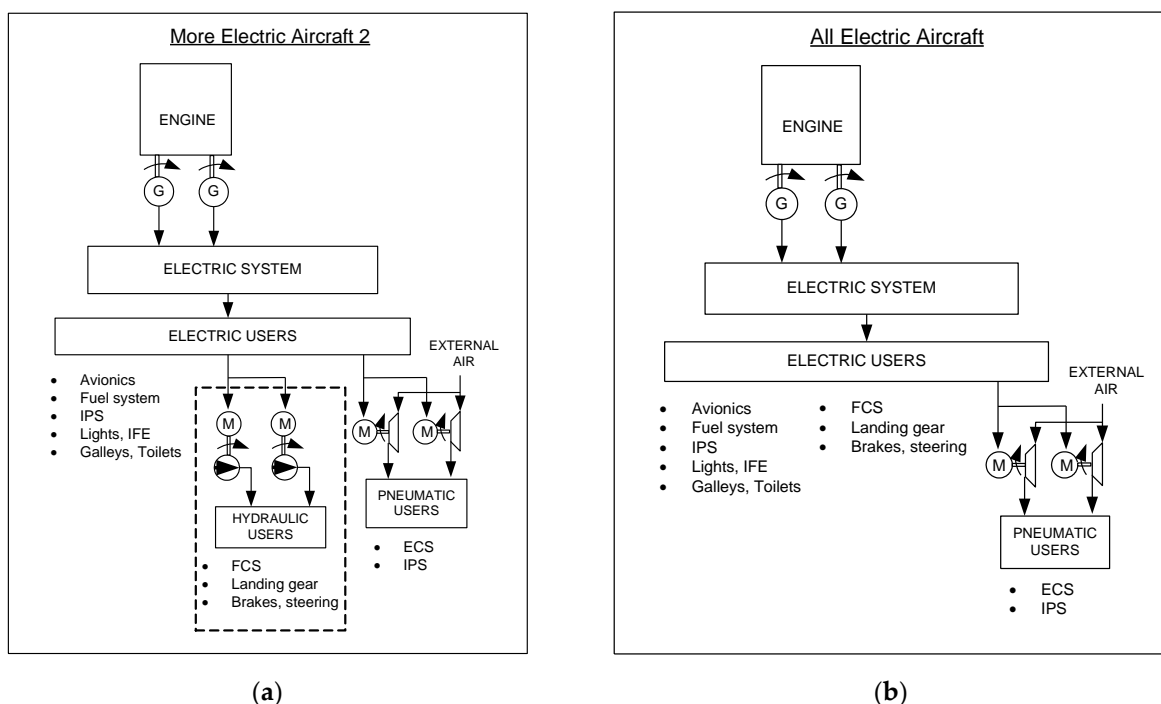
Figure 2. More electric n.2 (**a**) and all electric (**b**) OBS architectures.

The electrified pneumatic system is still used to provide power to the ECS. The IPS, that in the conventional architecture was a pneumatic user of the engine bleed system,

now relies on the electric pneumatic system. Due to the high electric power demanded by both the ECS and IPS, the EPGDS uses the same architecture as the MEA1, with high voltage (i.e., 270 VDC) busses and starter-generators. Finally, the HPGDS is not removed, but it is an electric user due to the use of Motor Driven Pumps (MDP) instead of EDP.

Finally, the AEA architecture depicted in Figure 2b includes the electrified systems of both the MEA1 and MEA2 architectures. Consequently, AEA reach the greater L_E since all the systems are powered by means of the EPGDS; no hydraulic or pneumatic power is directly required. This is achieved by removing the hydraulic actuation system and opting for high voltage EHAs. The ECS and IPS are connected to the electrified pneumatic system avoiding the need of any engine bleed system. All the mentioned systems, plus the engine starting system, are directly connected to the 270 VDC bus of the EPGDS. Only the avionics and some other small users need a DC-DC converter to be supplied by means of the low voltage bus (28 VDC).

3. Implementation of the Design Workflows

To investigate the effect on global and systems results when the OBS discipline is not integrated, or it is partially or fully integrated, three different MDA workflows are here proposed. Each workflow is defined within the RCE environment (Remote Control Environment (RCE). Retrieved 14 March 2022 online, website: https://rcenvironment.de/) and connects tools established and stored in different universities and research centers. The tools are connected to each other by means of an .xml file called CPACS (Common Language for Aircraft Design (CPACS). Retrieved 14 March 2022 online, website: http://cpacs.de/), already modified in previous research activities [18] to be compatible with OBS integration.

3.1. Disciplinary Competences

The disciplinary competences included in the workflows are described in this section.

3.1.1. OpenAD

OpenAD is an overall aircraft conceptual design tool developed by the DLR Institute of System Architectures in Aeronautics in Hamburg [19]. Used in several projects [20,21], it aims to provide a multidisciplinary and multifidelity design environment for aircraft design to evaluate and assess various concepts and technologies at aircraft level. It is based on the well-understood and mostly publicly available handbook methods (Luftfahrttechnisches Handbuch (2022 January 15). Retrieved 14 March 2022 online, website: https://www.lth-online.de/) [7,8,22–24], and on personal methods for disciplines for which no adequate or only insufficient methods could be sourced from the literature [25]. OpenAD, object-oriented programming in the Python scripting language, is a key enabler tool to generate a consistent initial evaluation of an air vehicle design. The current design space is valid for aircraft from commuter aircraft (e.g., Dornier 228) up to 800 passengers (e.g., A380), with enhanced capabilities on the design and thermodynamic cycle calculation of turbofan and turboprop engines. Dedicated to tube and wing concepts, the software offers wide capabilities to design, among other parts, strut braced wings, canards, and fuselage mounted engines in any combination. To achieve a consistent design, a minimum set of Top-Level Aircraft Requirements (TLARs) and design parameters have to be set. Focusing on the TLARs, it is mandatory to assign the design range, the cruise altitude, the Mach number, the payload, the reserve mission, the take-off field length, and the landing field length. Instead, within the design parameters, decisions related to the configuration of the aircraft components have to be made. For example, for the initial sizing, the design parameters for wing loading and the thrust-to-weight ratio are usually specified or varied as a design of experiment or optimization target among others. In case no decisions are made, OpenAD is set to design, as a default, a conventional aircraft configuration such as the Airbus A320 or the Boeing 737. However, calibration factors and design

constraints can be defined in the tool input to design new aircraft configurations. In this case, the masses, center of gravity and geometry of each component will be adjusted due to the set-up parametrization. To conclude, starting from the TLARs and design parameters, OpenAD generates a CPACS output file where the relevant aircraft data are exported according to the CPACS schema. Instead, additional output can be stored into the tool specifics.

3.1.2. ASTRID

ASTRID is a tool dedicated to OBS design developed at Politecnico di Torino [26]. As depicted in Figure 3, it is composed of the aircraft conceptual design and OBS design modules. The first module was not used as the conceptual design results are already available from OpenAD. Starting from the main aircraft masses, dimensions and performance, and additional information at the OBS level (e.g., the desired architecture, bus voltages, hydraulic system pressure, etc.), ASTRID calculates the loads and functions that each utility system must satisfy. The design of the utility systems (i.e., FCS, ECS, LGS, avionics, etc.) is carried out for each phase of the mission profile, delivering systems mass, dimensions and the power required. The power requirements are then used to design the electric, pneumatic, and hydraulic power generation and distribution systems. Finally, the mass of all the OBS, their volumes and the global engine offtakes are obtained.
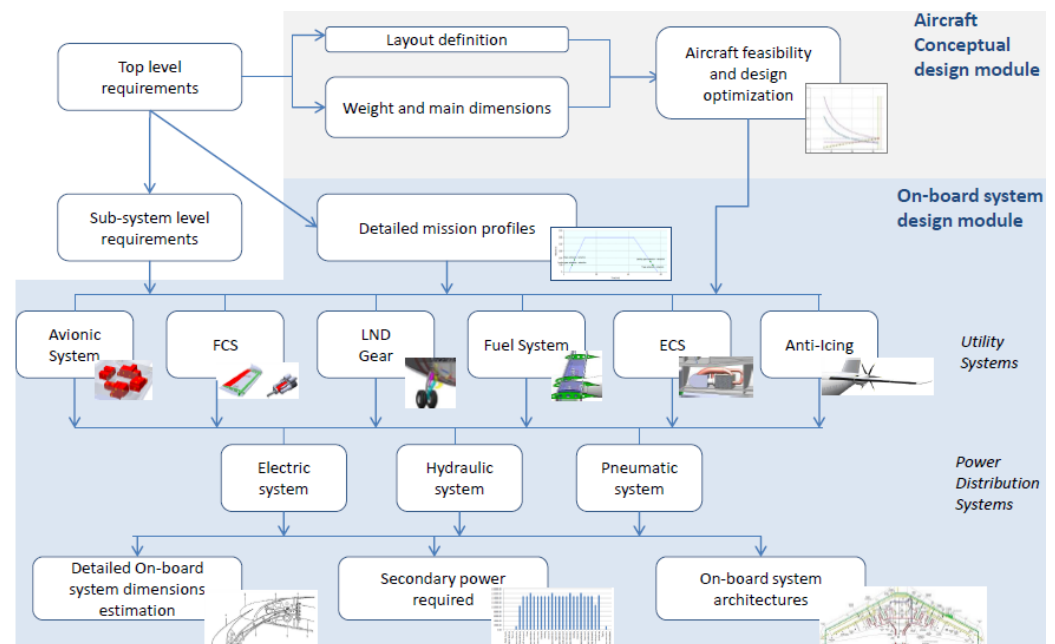
Figure 3. ASTRID OBS design process.

These results are obtained at the main equipment level and for each phase of the mission. The tool is able to design standard and different types of MEA and AEA architectures.

3.1.3. Performance

Aircraft performance tool is a simulation-based software which allows whole aircraft on-ground and in-flight calculations, including cruise, take-off, landing, climb, block fuel and time, and emissions performance. It uses a set of functionalities of the JPAD (Java Programming for Aircraft Design) library [27–30], an object-oriented API suitable for aircraft design, analysis, and optimization, whose core-pattern is depicted in Figure 4.

The input data needed are referred to the required characteristics (aircraft drag, at least in clean take-off and landing conditions), the available characteristics (installed thrust, fuel consumption and emission indices, at different flight ratings, altitude, and

Mach number), the lift characteristics (at least in clean take-off and landing conditions), and the design weights (at least in maximum take-off).

The take-off calculation module computes the whole take-off performance using a simulation-based approach, as stated in [28–30]. The analysis procedure expects to solve an appropriate set of Ordinary Differential Equations (ODE), which describes the aircraft equations of motion during the whole take-off phase up to the obstacle. The balanced field length is computed in case of OEI (one engine out condition). Here, the accelerate go and accelerate stop distances are simultaneously computed (solving similar ODE systems) and the balanced field length obtained where these distances are equal.

Figure 4. JPAD core-manager calculator pattern—example of take-off performance, courtesy of Trifari [30].

Similar to the take-off, a simulation-based approach, involving the resolution of an ODE system, is also used for the landing phase. The simulation starting point is assumed at 1500 ft above the runway and a stabilized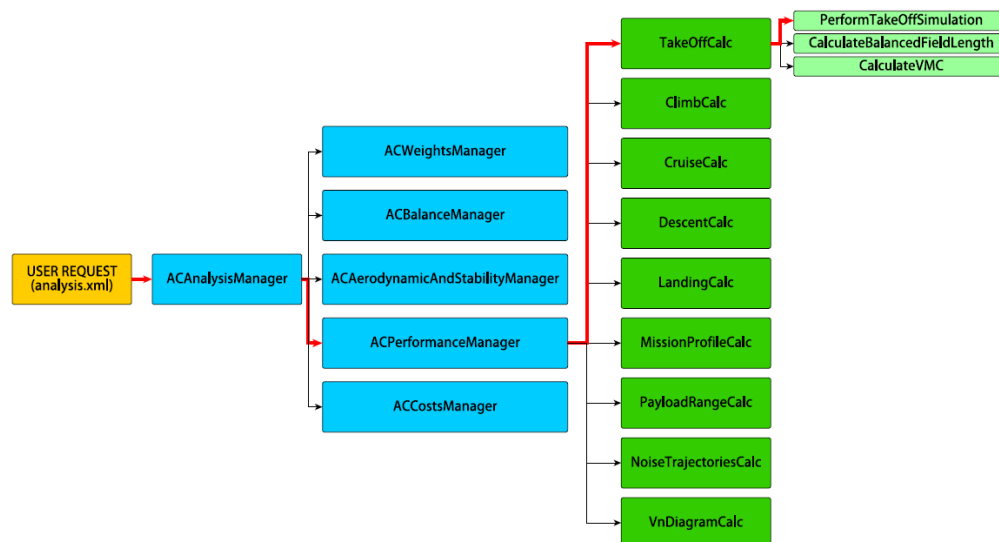 approach is employed, with a constant flight path angle and a calibrated airspeed maintained up to the obstacle height over the runway. From the landing obstacle altitude (50 ft), the aircraft begins the final approach down to the initial flare rotation. During the flare rotation, a smooth transition from a normal approach attitude to a landing attitude must be accomplished by gradually rounding out the flightpath to one that is parallel with, and within a very few inches above the runway. During this rotation, the angle of attack increases, providing for higher lift as well as induced drag, resulting in a deceleration of the aircraft. At the end, the aircraft must touch the ground with its main landing gear and with a reasonably low value of vertical speed. After the touchdown, after a few seconds of wheel free-roll, the pilot must apply a braking action of all the wheels brakes, deflect all the spoilers and set each engine setting to ground idle. The simulation ends when the aircraft speed reaches a value of zero.

The reason that climb performance is computed is twofold: the first is to evaluate the best climb performance of a given aircraft (rate of climb, glide ratio, ceiling in AEO and OEI conditions); the second to exactly compute the mission parameters (fuel consumed, range and time). In the second mode, the calibrated airspeed (CAS), the aircraft rate-of-climb (ROC) and the initial cruise altitude must be specified, and, if not reachable, the tool switched to the best rate of climb condition and practical ceiling altitude.

Cruise performances are computed to evaluate the aircraft flight envelope and the mission profile cruise segment (fuel flow and distance covered). In the second case, the cruise altitude, the desired Mach number, and the cruise mode must be specified (fixed or variable altitude). If some parameters are violated, the tool computes the cruise performance at the cruise ceiling altitude and the maximum achievable Mach number.

From the prescribed final cruise altitude, descent performance is computed to evaluate the fuel flow and the range of the descent phase. The CAS and the rate-of-descent (ROD) must be prescribed, and if violated, the tool uses the minimum ROD condition.

Block fuel, block range and block time data are computed iterating take-off, climb, cruise, descent, and landing segments coherently to the prescribed input data described previously (altitude, speeds, ROC, ROD, etc.). In the design mode, the tool is also capable of adding the eventual alternate, loiter, and reserve phases. A schema of the mission profile analysis is shown in Figure 5, highlighting the inner loops to converge on the required specifications. The main objective is an accurate calculation of block fuel, time, and emissions.
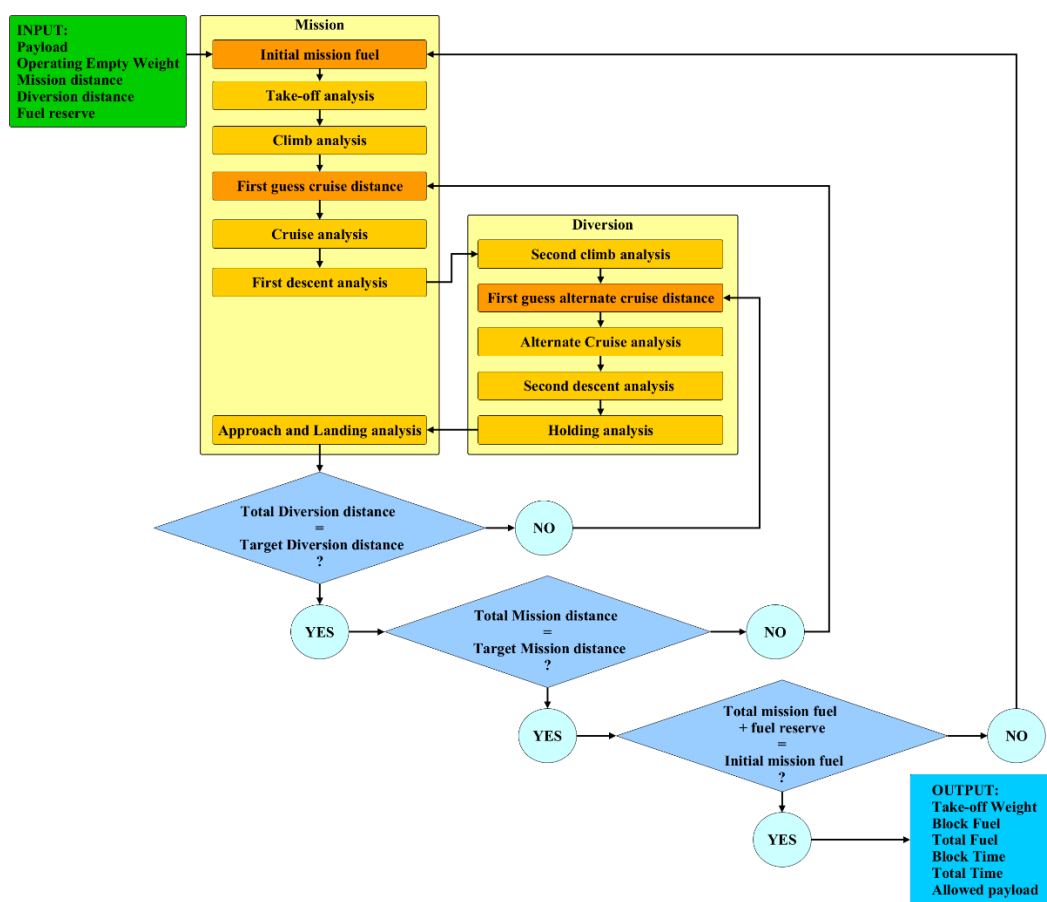
Figure 5. Flowchart of the mission profile analysis performed by JPAD, courtesy of Trifari [30].

3.1.4. Engine

Engine modelling is crucial for performance evaluation. The Engine tool is suitable to design an engine deck, providing thrust or power characteristics, fuel consumption, emissions indices, masses, and geometry. The tool needs as inputs the required thrust for several ratings (top of climb, take-off, cruise) and the engine type (turbofan, turboprop), and provides as outputs the engine maps, in terms of thrust versus Mach, altitude, throttle ratings and the temperature condition. These maps are obtained with GASTURB ((Online). Available: https://www.gasturb.de/index.php. (Accessed 14 March 2022)) software. The tool is also able to rubberize the designed engine, in a range of ±20% of the maximum thrust or power. Finally, the tool also provides an estimation of the engine dry mass and the main geometrical characteristics.

3.1.5. SFC Sensitivity

The tool, provided by the Politecnico di Torino, is capable of calculating the effect of power offtakes on engine Specific Fuel Consumption (SFC). It is based on a scalable engine deck of turboprop engines. The main inputs are the basic SFC, provided by the engine design tool, and the power offtakes and air-bleed requirements provided by the ASTRID tool. The basic SFC is used as a reference point to generate a new SFC value, collecting the adverse effects of providing the additional mechanical power and compressed air required by OBS. The tool is able to differentiate between the increase in SFC due to power offtakes and due to bleed requirements. Therefore, the tool can be used to evaluate the different OBS architectures that have a different balancing of required mechanical power and bleed air.

3.1.6. Aircraft Synthesis

As widely explained above, OpenAD is a software tool for preliminary aircraft design used to generate a CPACS output file, including the relevant data of an aircraft, starting from the TLARs and the design parameters. Nevertheless, distributed collaborative design workflows usually include analysis capabilities of different levels of modelling fidelity. These broader design environments are required not only as providers of initial solutions, but also as tools able to dynamically adapt to the results provided by the disciplinary tools, performing the required synthesis calculations. OpenAD is an essential part of the multidisciplinary and multifidelity design workflow since it is used to derive an initial design as well as to synthetize higher fidelity disciplinary results into the design. Differently from the OpenAD initializer, in this case, the main inputs for OpenAD are the design parameters estimated by other high-fidelity tools. A CPACS output file, assessed on these new design parameter values, is the main output of the OpenAD aircraft synthesis.

3.2. Analysis Workflow Definition

After the description of the tools involved, it is now possible to define the workflows proposed. Each of them represents a different level of OBS integration. From their results, it is possible to understand the effects, at aircraft design level, of the OBS integration and systems electrification.

3.2.1. Workflow 1

The first workflow tested (see Figure 6) represents a simple connection of the aircraft conceptual design discipline (i.e., OpenAD tool) with the OBS design (i.e., ASTRID tool). Here, the OBS masses assumed in the conceptual design phase by means of percentages of operating empty mass (OEM) are overwritten with the results from a preliminary design of the OBS. No converging loop is here considered; therefore, the snowball effect is not taken into account. However, the aircraft global masses have been made consistent after the ASTRID calculation. Without the presence of a converging loop and the recalculation of the aircraft performance and masses, this basic workflow can be considered as a reference of an aircraft design where the OBS discipline is executed but not actually integrated. The only integration is represented, as depicted in Figure 6, by the great number of parameters regarding aircraft geometry, mass and performance used as inputs for the OBS preliminary design.
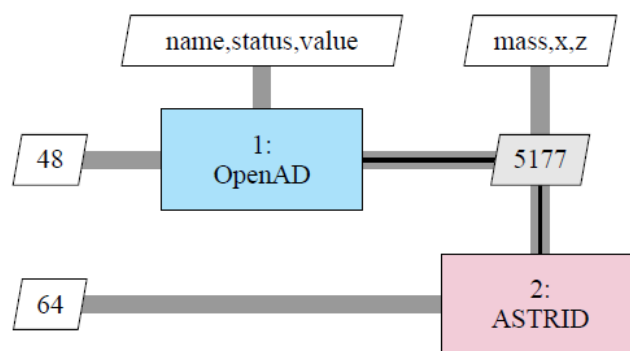
Figure 6. First workflow tested—OBS not integrated.

3.2.2. Workflow 2

The second workflow (see Figure 7) represents a partial integration of the OBS discipline in the whole aircraft design. The aircraft conceptual design module (i.e., OpenAD) is used to initialize the converged MDA. After the OBS preliminary design, two other tools are employed to calculate the performance and to design the engine with a greater fidelity compared to the conceptual design. Moreover, these two additional tools are initialized with the new aircraft masses that consider the OBS masses coming from ASTRID. After the calculation of flight performance and the engine mass and geometry, the MDA is reiterated until MTOM convergency. This represents a first example of OBS integration that is focused only on mass parameters. This means that the effect produced by the OBS masses is considered by the new masses of the engine and on aircraft performance (i.e., fuel mass).
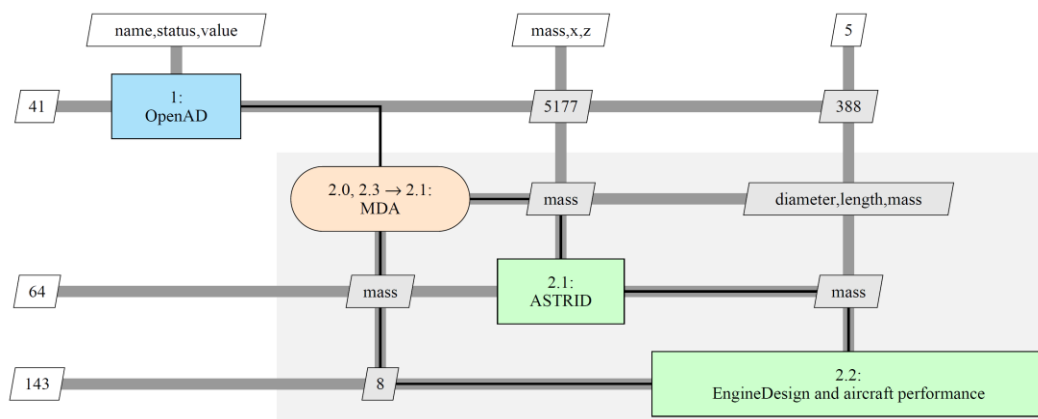
Figure 7. Second workflow tested—OBS partially integrated.

3.2.3. Workflow 3

In the third workflow proposed (see Figure 8) the SFC sensitivity tool is added. This tool is included inside the MDA convergency loop and executed after the engine design. An important variable of OBS architectures is the power requirement. The SFC sensitivity tool is able to define a new engine SFC depending on the system's power offtakes and the bleed air required. Since the system's power requirement changes during the mission, for each mission phase a new SFC is provided. Following the workflow implementation and additionally to the second workflow, the OBS design also provides power requirements for each mission phase. The SFC sensitivity tool modifies accordingly the engine SFC used in both the performance and the engine design tools. In this way, the additional fuel burnt due to the OBS power requirement and the secondary effect of reducing engine efficiency (i.e., increasing engine SFC) is taken into account during the mission performance calculation.
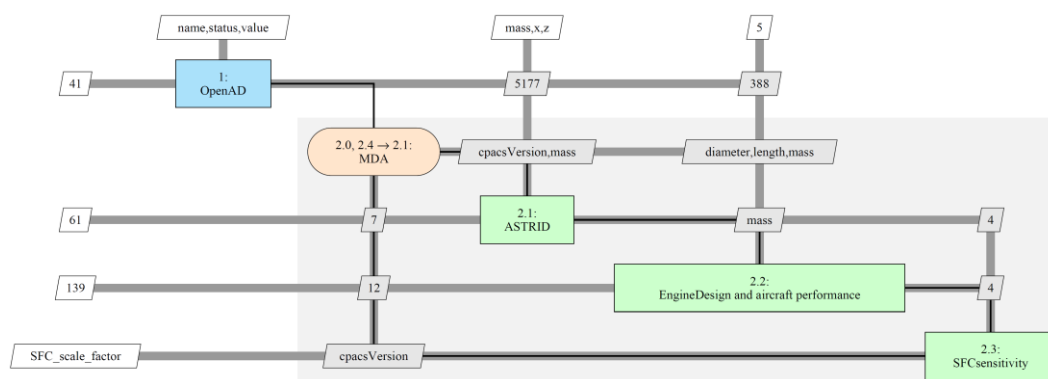
Figure 8. Third workflow tested—OBS partially integrated.

3.2.4. Workflow 4

Lastly, in the fourth and final workflow, depicted in Figure 9, the aircraft airframe and geometry redesign is added in the MDA converging loop. Therefore, the Aircraft Synthesis tool enables the full integration of the OBS discipline, allowing for the complete snowball effect of the aircraft masses. From the OBS design prospective, this workflow allows the influence of the different architectures on the airframe and engine mass, and on aircraft performance, to be quantified. Moreover, the influence on the fuel consumption is fully considered, quantifying both the mass variation due to a different aircraft mass and a different effect on engine SFC. It is worth noting that by changing the OBS architecture, the small mass variation is propagated at aircraft level, redesigning it. Therefore, for each architecture a slightly different aircraft is obtained. However, each of them is compliant with the TLARs listed in Table 1.
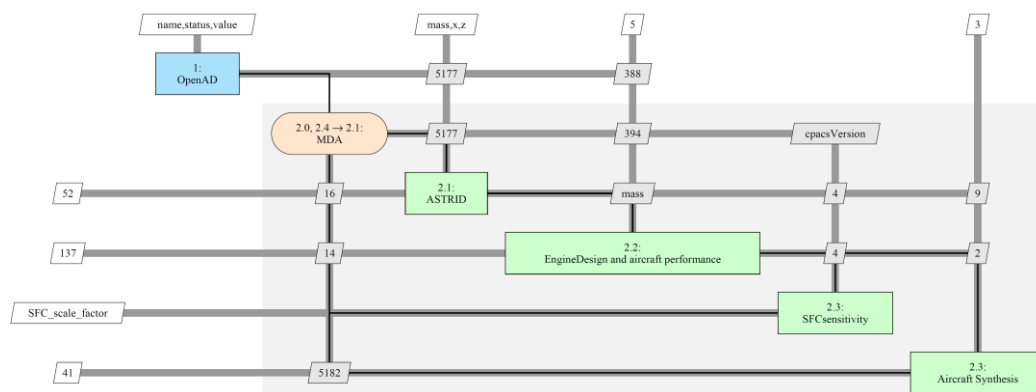
Figure 9. Fourth workflow tested—OBS fully integrated.

4. Results and Discussions

Before focusing on the different results obtained by running the different workflows, the results of OAD and performance are shown. The multidisciplinary and multifidelity workflow starts with OpenAD, the conceptual aircraft design tool. It is used to obtain the reference aircraft baseline, and thus, all the main aircraft data, starting from the TLARs.

4.1. Reference Aircraft

The reference aircraft is a small regional turboprop aircraft, carrying 19 passengers from airports with relatively short runways (TOFL of 800 m), flying with a cruise speed of 0.45 Mach at 7620 m. It can be used to connect small airports to each other or to a hub, also at large distances, having a range of 1500 km. These TLARs, summarized in Table 1, are the inputs needed from OpenAD to run. However, other configurational decisions must be taken on some design parameters to obtain the desired baseline. The vertical

position of the wing, with respect to the fuselage and the engines allocation, is one example. In fact, as a default, OpenAD is set to design a conventional aircraft configuration such as the Airbus A320 or the Boeing 737. However, differently from these, for this reference aircraft a high-wing layout has been adopted for similarity with other 19-pax aircraft configurations, i.e., the Dornier 228. In addition, the relative engine's x-position with respect to the wing is set to zero. In this way, the engines are directly mounted under the wing, not having the need for pylons. The fuselage layout, chosen as elliptical, is another additional design parameter provided as an input to OpenAD.

The reason for this choice relates to the need for pressurization due to the altitude at which the aircraft must fly. This aspect differentiates this reference aircraft from other 19-pax aircraft configurations, like the Dornier 228 or Beechcraft 1900, usually flying at lower altitude, and thus characterized by a square fuselage layout. Moreover, slats and spoilers have not been included in the OpenAD inputs since these components are usually not adopted by 19-pax aircraft configurations. Provided with the TLARs and the specified additional design parameters as inputs, OpenAD generates the reference aircraft baseline whose three views are shown in Figure 10. Some representative aircraft specifications are instead reported in Table 2. As required, this aircraft is compliant with the C23, showing an MTOM of about 8.5 tons.
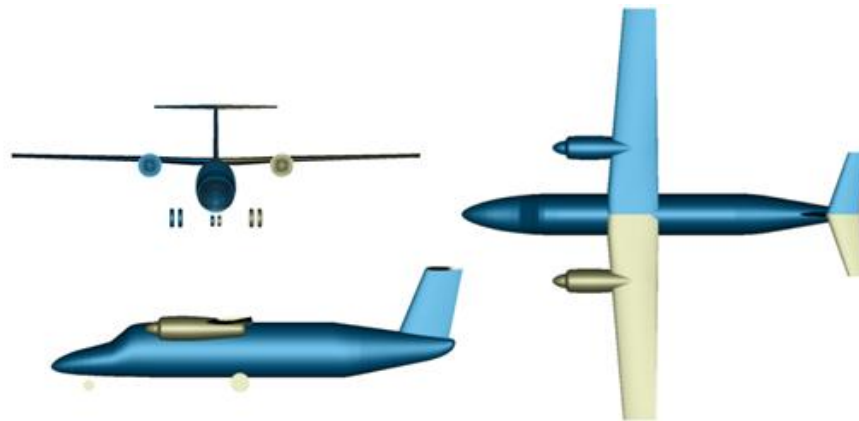
Figure 10. Three views of the reference aircraft.

Table 2. Specification of the reference aircraft.

Specifications	Value	Unit
N Pilots	2	-
N Pax	19	-
Mass per Pax	93	kg
Max Payload	2052	kg
Design Range	1500	km
Design Payload	1976	kg
Design Cruise Mach	0.45	-
sTOFL	800	m
Cruise Altitude	7620	m
Wing Loading	265	kg/m^2
Power/MTOM	0.257	kW/kg
MTOM	8478	kg
OEM	5442	kg
MZFW	7495	kg

The results of OAD are also confirmed and refined by the performance tool. From the flight envelope, depicted in Figure 11a, it is worth noting that the aircraft reaches (and slightly exceeds) the required speed at the ceiling altitude. This is the design point for the propulsion system. For this reason, as shown in Figure 11b, the aircraft outperforms the take-off field length requirement. Therefore, the engines could be flat rated for ground operation. Moreover, the speed requirement leads to a greater real ceiling altitude as depicted in Figure 12a. However, as for other aircraft (e.g., Beechcraft 1900 d), the maximum ceiling is limited by the cabin pressurization at 7600 m. This decreases the fuselage mass since there is no need for this kind of aircraft to fly at higher altitude. Finally, Figure 12b shows the aircraft meets the maximum range requirement of 800 nm.

(a)

(b)
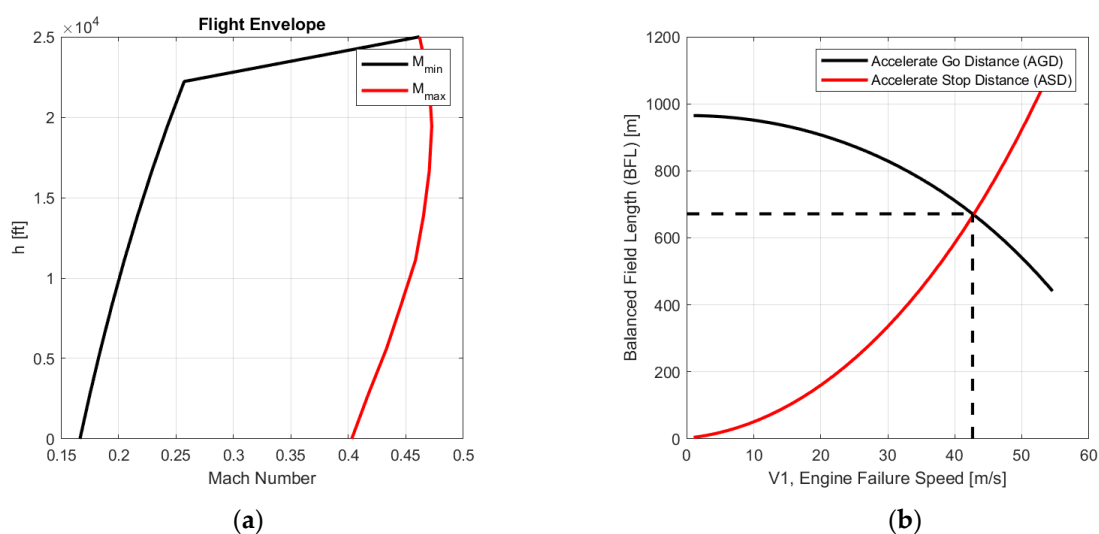
Figure 11. (**a**) Aircraft envelope and (**b**) balanced field length.

(a)

(b)
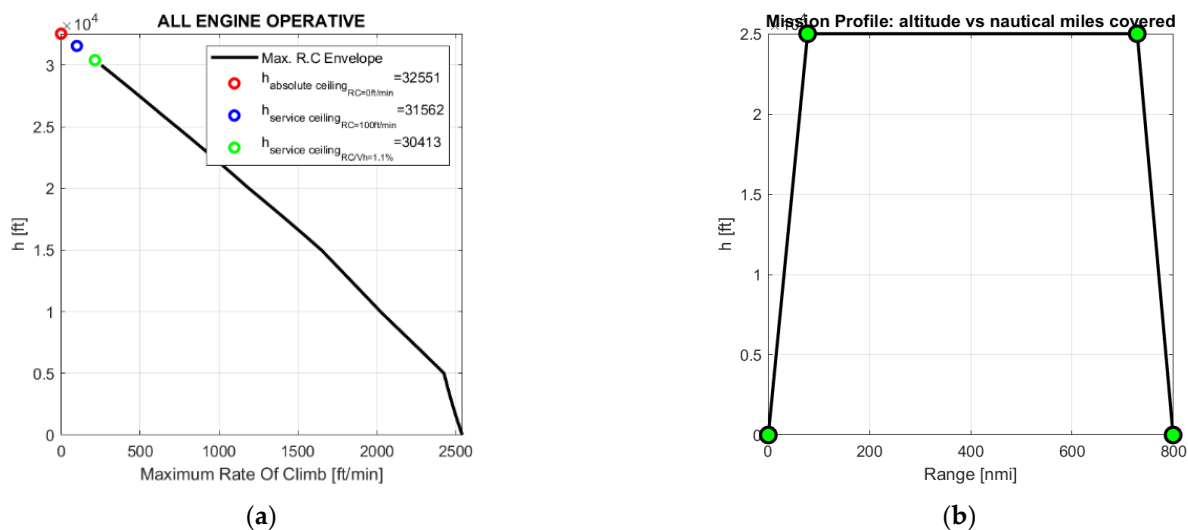
Figure 12. (**a**) Rate of climb and (**b**) mission profile.

4.2. Workflow Comparisons

The main results are summarized in terms of aircraft masses and the OBS masses in Table 3 individually for each of the four workflows. Moreover, for each workflow, four columns are defined to list the results of the four OBS architectures. In this way, it is possible to investigate both the effect of systems electrification and the different results obtained by increasing the integration of the OBS design with the other disciplines. It is

worth noting that the OBS masses change with the architecture, but they are practically constant with the integration level. This means that the OBS is certainly sensitive to its architecture, but a smaller effect is inherited from the other disciplines since the aircraft TLARs remain constant. Focusing on OBS masses in all the workflows it is possible to note:

- The mass of the systems that do not participate in the electrification (e.g., avionics, furnishing, fire protection, oxygen, and lights) remain constant.
- The electrification of the actuation systems of the flaps and the landing gear slightly increases the mass of these systems due to the greater mass of the EHAs compared to the hydraulic actuators.
- An increase in the mass of the ECS and IPS can be noticed for the electrified architecture. This is mainly due to the use of additional components (i.e., electric motor compressors).
- The electrification only partially increases the EPGDS mass since the use of high voltage components partially dampens the increase in mass due to the use of more powerful components.
- The main advantage of the electrified architectures is given by the removal of the HPGDS and/or the PPGDS that always produces a reduction in the total systems mass.
- Finally, the OBS electrification always produces a beneficial effect in terms of mass reduction. MEA1 is the lightest architecture followed by the AEA and MEA2.

Considering now the results at aircraft level, a variation can be noticed when comparing the architectures and the different workflows. Since the rationale is different for the two variations, they are addressed separately. Firstly, the different influences of the OBS electrification on the entire aircraft are explained, and then the changes in the global results for each workflow are addressed. To explain the influence of the OBS electrification, it is more convenient to focus on the results of the fourth workflow which covers all the OBS influences on the overall aircraft design.

Table 3. Results of the four MDA workflows.

Masses (kg)	Workflow n.1				Workflow n.2				Workflow n.3				Workflow n.4			
	Conv	MEA1	MEA2	AEA	Conv	MEA1	MEA2	AEA	Conv	MEA1	MEA2	AEA	Conv	MEA1	MEA2	AEA
MTOM	8630	8470	8564	8495	8633	8456	8563	8484	8619	8438	8530	8452	8620	8394	8511	8413
ZFW	7647	7486	7580	7511	7633	7464	7565	7491	7563	7391	7490	7416	7660	7454	7570	7482
OEM	5595	5434	5528	5459	5581	5413	5513	5439	5587	5415	5514	5440	5608	5402	5518	5430
Airframe	n.a.	n.a.	n.a.	n.a.	n.a.	n.a.	n.a.	n.a.	n.a.	n.a.	n.a.	n.a.	2356	2326	2342	2328
M_FUEL	n.a.	n.a.	n.a.	n.a.	1058	1049	1055	1050	1056	1046	1040	1036	1063	1042	1043	1033
Operator items	468	468	468	468	468	468	468	468	468	468	468	468	468	468	468	468
Tot sys + Operator items	2108	1948	2041	1973	2100	1930	2029	1956	2100	1930	2029	1956	2101	1927	2028	1953
Avionics	135	135	135	135	135	135	135	135	135	135	135	135	135	135	135	135
FCS	141	144	141	144	142	144	141	144	142	144	141	144	142	143	141	143
IPS	68	68	72	72	68	68	72	72	68	68	72	72	69	68	72	72
ECS	107	107	129	129	107	107	129	129	107	107	129	129	107	107	129	129
Fuel systems	55	55	55	55	40	40	39	39	40	40	39	39	40	40	40	39
LNDG	332	354	332	354	337	353	334	353	337	353	334	353	337	351	333	352
Furnishing	820	820	820	820	821	819	820	820	821	819	820	820	821	819	820	819
Fire protection	10	10	10	10	10	10	10	10	10	10	10	10	10	10	10	10
Lights	68	68	68	68	68	68	68	68	68	68	68	68	68	68	68	68
Oxygen	24	24	24	24	24	24	24	24	24	24	24	24	24	24	24	24
Water Waste	0	0	0	0	0	0	0	0	0	0	0	0	0	0	0	0
APU	0	0	0	0	0	0	0	0	0	0	0	0	0	0	0	0

PPGDS	56	56	0	0	56	56	0	0	56	56	0	0	56	56	0	0
HPGDS	99	0	94	0	99	0	94	0	99	0	94	0	99	0	94	0
EPGDS	194	107	163	163	194	107	163	163	194	107	163	163	194	107	163	163

In Figure 13, these results are depicted in terms of a comparison of the electrified architectures with the conventional one. The following results are obtained:

- Due to the complete removal of the HPGDS, the MEA1 and the AEA achieve a reduction in systems mass of about 8% and 7%, respectively;
- AEA architecture is able to reach the highest fuel mass saving (2.8%) due to the sum of two contributions: MTOM reduction due to OBS mass reduction and engine SFC enhancement due to the use of the bleedless technology. It is worth noting that MEA1 and MEA2 enable the same two contributions but separately. The reduction in fuel mass for MEA1 (2.0%) is only due to the lighter OBS, whereas for MEA2, the fuel reduction (1.9%) is mainly due to the use of bleedless technology. The effect of the two contributions on fuel saving is not linear and the overall effect cannot be represented by a simple sum of the individual contributions.
- Considering the mass distribution for this kind of aircraft, the mass saving obtained by electrifying the OBS is dampened for the other aircraft components (e.g., the airframe mass) and for the whole aircraft (e.g., OEM, MTOM, etc.). For example, the OBS mass saving of 8.3% achieved by MEA1 produced an MTOM reduction of 2.6%.
- Finally, considering the reduction in MTOM, the advantage obtained by adopting MEA1 and AEA architectures is similar. MEA2 is only able to achieve half of the mass saving of the other electrified OBS.

It is worth noting that the advantage of using the bleedless engine technology employed in MEA2 and AEA is strongly connected with the aircraft mission duration. The reduction in engine SFC could produce a greater fuel reduction in long haul aircraft entailing a bigger MTOM saving [18]. Therefore, the results presented here are dependent on the aircraft category.
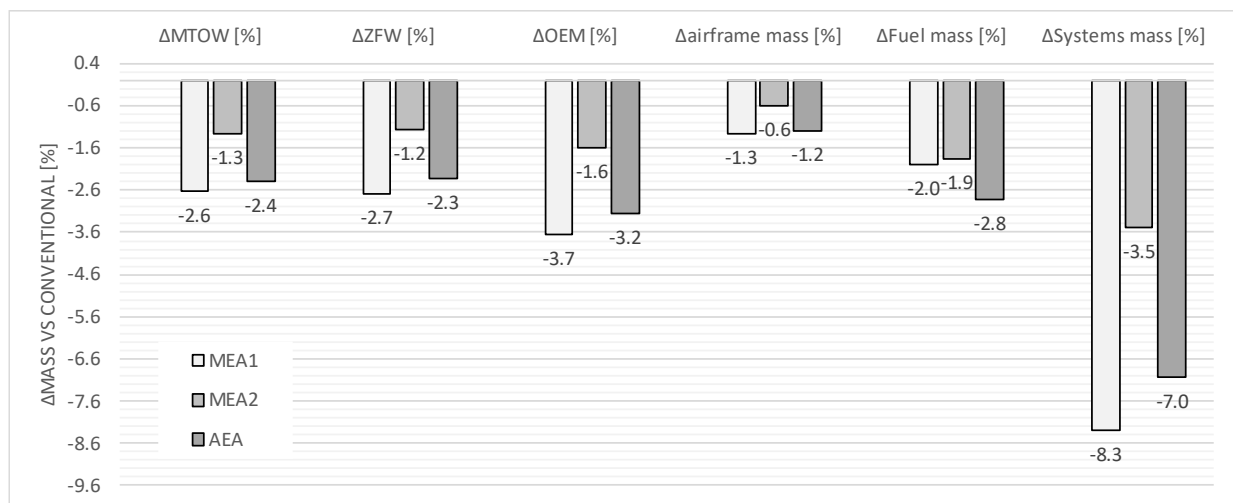

Figure 13. Comparison between conventional architecture and MEA1, MEA2 and AEA (results from workflow n.4).

In Table 4, the mechanical power and the pneumatic airflow required by each architecture during the different mission phases are listed. The results, obtained by the complete workflow (i.e., workflow n.4), primarily show the absence of pneumatic power requirements for MEA2 and AEA architectures that use the bleedless technology. It is also worth noting the huge increase in mechanical power required by those architectures during all the mission phases. Despite this, the adverse effect on engine efficiency is lower

than the conventional and MEA1 architectures, as previously seen in terms of fuel consumption.

Figures 14 and 15 show, in an explicit way, the trends of the mechanical power offtakes and the pneumatic airflow requirements, respectively, within the mission. As it is clearly understandable by the two graphs, the least power demanding phase is the cruise. The other phases are affected by hot day conditions—the worst case for the ECS. Therefore, considering that the ECS represents the most power demanding system, the trend of the power requirements is essentially determined by its behaviors.

Table 4. Power requirements of the conventional architecture and MEA1, MEA2 and AEA (results from workflow n.4).

|	Mission Phase	Mechanical Power (W)				Pneumatic Airflow (kg/s)			
		Conv	**MEA1**	**MEA2**	**AEA**	**Conv**	**MEA1**	**MEA2**	**AEA**
1	Pre—flight checks	5410	5402	50,999	50,999	0.25	0.25	0	0
2	Engine start-up	7162	6886	52,482	52,482	0.25	0.25	0	0
3	Taxi out	13,415	14,336	60,564	60,513	0.25	0.25	0	0
4	Taxi out—flaps down	13,111	13,928	60,235	60,104	0.25	0.25	0	0
5	Take off—run	13,029	14,104	60,275	60,275	0.25	0.25	0	0
6	Take off—manoeuvre	13,029	14,104	60,263	60,263	0.25	0.25	0	0
7	Take off—lnd gear up	15,396	15,563	62,847	61,675	0.25	0.25	0	0
8	Take off—flaps up	13,657	14,534	61,123	61,044	0.24	0.24	0	0
9	Climb	13,686	14,702	63,913	63,913	0.11	0.11	0	0
10	Cruise	8149	8254	35,479	35,479	0.12	0.12	0	0
11	Descent	13,544	14,530	63,692	63,692	0.11	0.11	0	0
12	Descent—flaps down	14,039	14,822	62,410	62,331	0.23	0.23	0	0
13	Approach—lnd gear down	13,142	14,221	61,389	61,389	0.23	0.23	0	0
14	Approach	13,139	14,217	60,847	60,847	0.24	0.24	0	0
15	Landing—manoeuvre	13,029	14,104	60,265	60,265	0.25	0.25	0	0
16	Landing—run	13,861	15,378	61,207	61,561	0.25	0.25	0	0
17	Taxi in—flaps up	9539	9323	55,050	54,919	0.25	0.25	0	0
18	Taxi in	9020	9006	54,654	54,602	0.25	0.25	0	0
19	Engine shutdown	5631	5670	51,266	51,266	0.25	0.25	0	0
20	Emergency	14,001	14,783	29,157	29,077	0.08	0.08	0	0
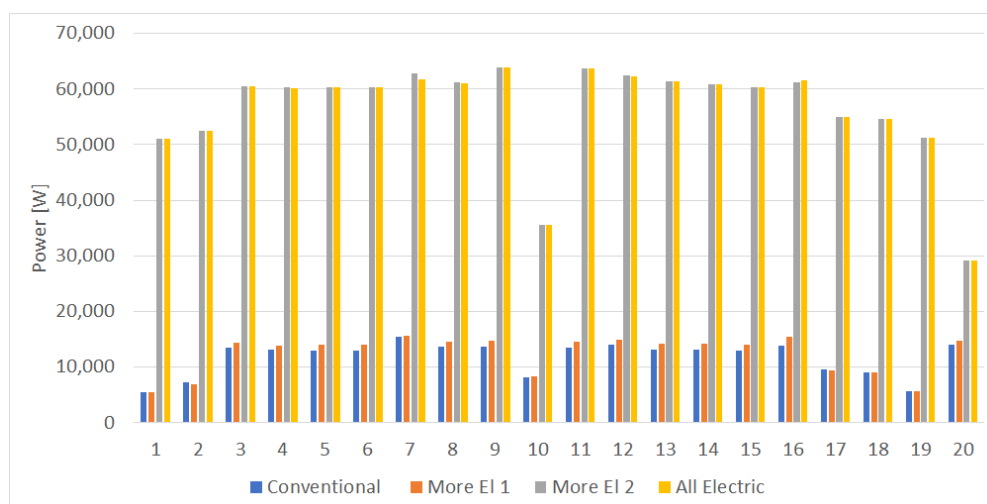
Figure 14. Mechanical power offtakes for the four OBS architectures (results from workflow n.4).
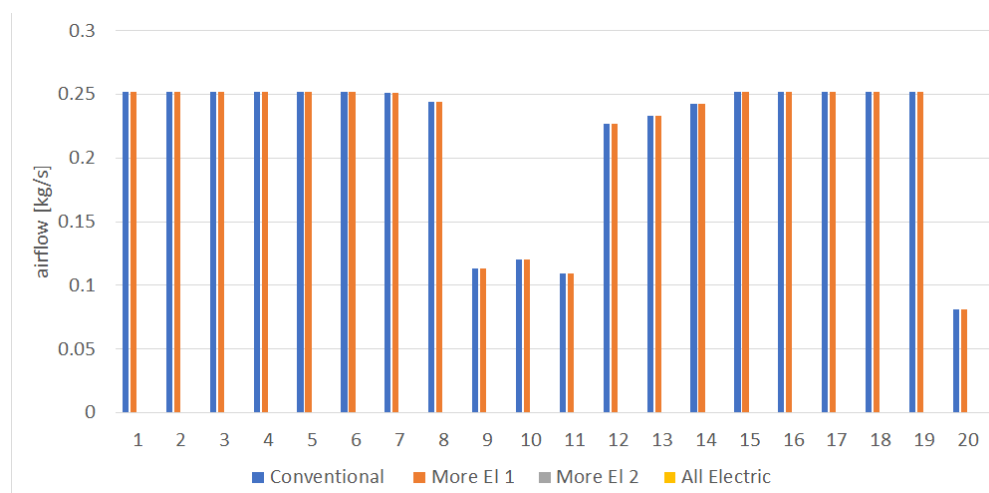
Figure 15. Pneumatic airflow requirement for the four OBS architectures (results from workflow n.4).

A second important achievement is the variation of the results by changing the OBS integration with the other design disciplines. In this way, it is now possible to quantify the possible error in evaluating the different OBS architectures with disciplines with inadequate integration between them. From Figure 16, it is possible to see the increasing difference, in terms of MTOM variation, between the OBS architectures when the integration level is increased by enhancing the employed workflow. This means that by using a workflow where the OBS discipline is not fully integrated, the possible advantages obtained from OBS electrification are not completely captured. Comparing the results of workflow n.1, where the OBS discipline is not integrated, with the results of the other workflows, it is possible to obtain the diagram shown in Figure 17. Analyzing the diagram, the following points can be observed:

- Increasing the integration level, a variation of about 1% of MTOM can be observed when the results of workflow n.1 are compared with those of workflow n.4. A total of 1% of MTOM represents about 40% of the actual MTOM variation due to the different OBS architecture. This means that by using workflow n.1 an error of about 40% could be expected.
- For the conventional OBS architecture, the error is quite small when changing the integration level. It could be due to the assumptions considered in the other disciplinary tools that are already set for conventional systems. As a consequence, and looking at the variation for the other architectures, to correctly evaluate innovative systems, a workflow with a higher level of integration is necessary.
- Among the integrated disciplines, the SFC variation due to the OBS power offtakes represents an important improvement in the results, as shown in Figure 17 for workflow n.3. This is particularly true for the MEA2 architecture that in workflow n.2 produces the same effect as the conventional configuration.
- Finally, the aircraft redesign, discipline added in workflow n.4, is the greater contributor to the correct integration of the OBS design. The airframe and geometry redesign produce a notable effect on all the other disciplines involved (aircraft performance and engine design). This time, the enhancement added with workflow n.4 improves the results of the MEA1 and AEA architectures, that entail the greater mass reduction that can be correctly inherited by the other aircraft components by means of the aircraft synthesis.
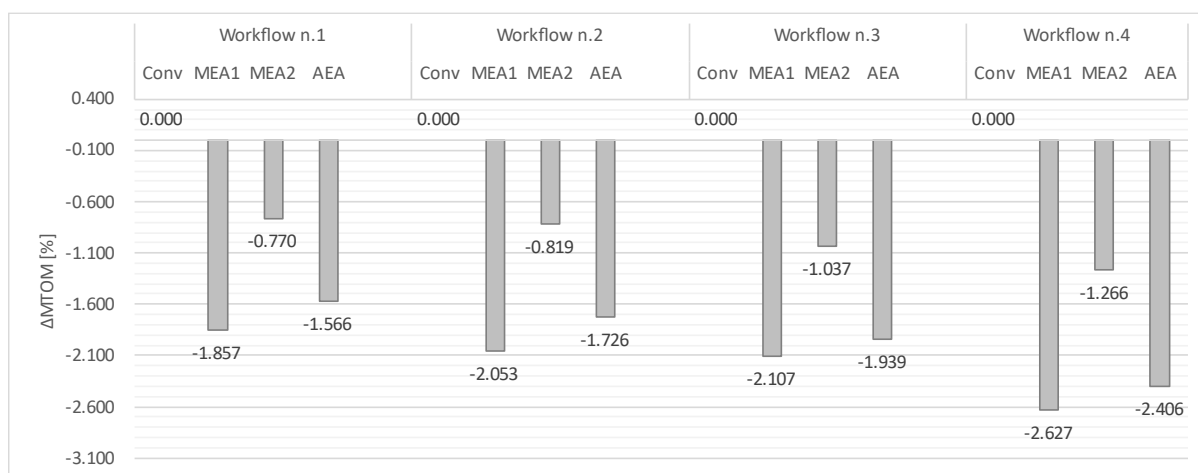
Figure 16. Different assessments of OBS architectures using the four workflows under study having as reference the conventional architecture.
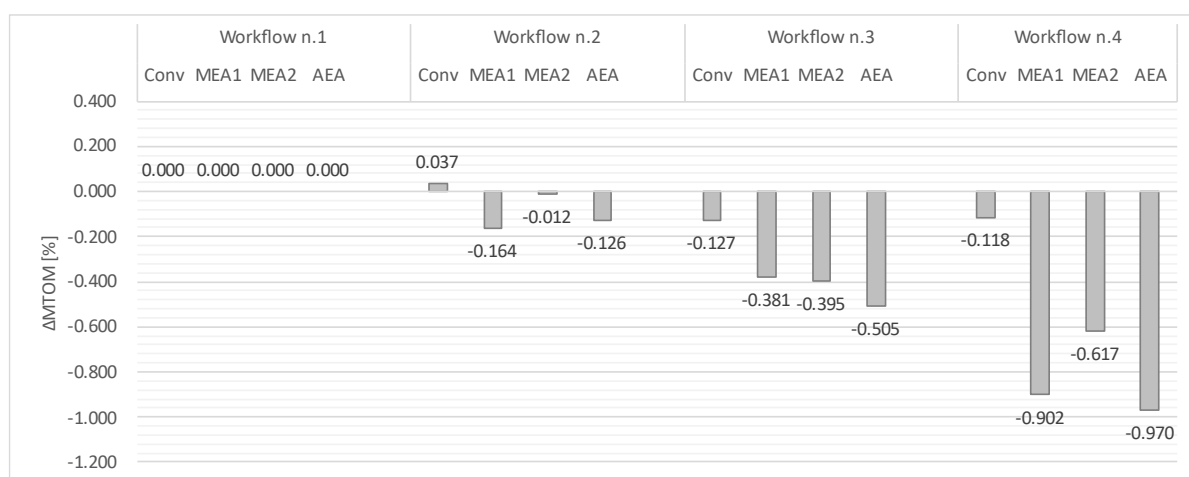

Figure 17. Different assessments of OBS architectures using the four workflows under study having as reference workflow n.1.

5. Conclusions

The present paper shows the importance of increasing the integration of the OBS design with the other disciplines, especially when a comparison among different systems architectures is needed. Four workflows, with an increasing level of OBS integration, are proposed and tested. Each workflow has been utilized to design a small regional aircraft, with fixed TLARs, and with four OBS architectures with different levels of electrification. The results demonstrate that the OBS design discipline is mainly connected with the others by two parameters: the systems mass and the system power requirement. The systems mass parameter should be captured by all the design disciplines of an MDO workflow (e.g., engine and airframe design, mission performance). The second parameter, the systems power requirement, should be taken into account by the engine design, considering the important influence on the performance of the propulsion system. The power requirement together with its influence on engine efficiency produces, in turn, an effect on fuel mass and hence on the mass of all the aircraft components.

Comparing the results of the different workflows in terms of aircraft MTOM, an error of about 40% on the OBS architectures' assessment has been found, when the OBS discipline is not fully integrated with the others. This happens mainly when electrified OBS architectures are considered. A lower error is encountered for the conventional system architecture since the workflow tools are inherently set for it. Therefore, by having the

electrified architectures' new influences on the other aircraft components and their performance, it is necessary to deeply integrate the workflow disciplines together to catch their mutual influences. Contrary to conventional OBS, for the electrified ones, these new influences cannot be assumed in the tools themselves.

Another interesting result of the present paper concerns the systems electrification. All electrified architectures provide advantages in terms of mass and fuel saving. In particular, the removal of the HPGDS greatly reduces the OBS mass, avoiding the installation of hydraulic pipes, fluid, and dedicated equipment not utilized by other systems. On the contrary, the electrification produces a synergic effect among the systems and the rise of the EPGDS mass can be dampened using high voltage technology. A reduction in MTOM of 2.6% is expected when those technological improvements are implemented, as in the MEA1 architecture. Another important step for OBS electrification is the use of the bleedless technology. For the aircraft category analyzed here, this does not produce an important mass improvement, but a more substantial fuel saving. The AEA architecture entails a reduction in MTOM of 2.4% but a reduction in fuel burnt of 2.8% (0.8% higher than MEA1).

Finally, possible improvements can be evaluated in future analyses. A secondary influence of OBS on the other design disciplines is related to the systems volume and the need for air flow for temperature control. The OBS volume has an effect on the aircraft shape (e.g., the landing gear and actuator fairings) and it changes according to the technology selected for each component. This would be a further integration in order to evaluate a difference in aircraft drag. In this way, the air intakes needed by OBS, especially the ones needed by the ECS, also differ with the electrification level and they have an additional influence on aircraft drag.

Conflicts of Interest: The authors declare no conflict of interest. The funders had no role in the design of the study; in the collection, analyses, or interpretation of data; in the writing of the manuscript, or in the decision to publish the results.

Abbreviations

The following abbreviations are used in this manuscript:

ACM	Air Cycle Machine
AEA	All Electric Aircraft
CAS	Calibrated Air Speed
ECS	Environmental Control System
EDP	Engine Driven Pump
EHA	Electro Hydrostatic Actuator
EPGDS	Electric Power Generation and Distribution System
FCS	Flight Control System
HPGDS	Hydraulic Power Generation and Distribution System

IPS	Ice Protection System
MDA	Multidisciplinary Design Analysis
MDAO	Multidisciplinary Design Analysis and Optimization
MEA	More Electric Aircraft
MTOM	Maximum Take Off Mass
OAD	Overall Aircraft Design
OBS	On-Board Systems
OEM	Operating Empty Mass
PPGDS	Pneumatic Power Generation and Distribution System
PPDU	Primary Power Distribution Unit
SFC	Specific Fuel Consumption
SPDU	Secondary Power Distribution Unit
TLARs	Top Level Aircraft Requirements
TOFL	Take Off Field Length
L_E	Level of electrification [-]
P_E	Total electric power generated [W]
P_T	Total non-propulsive power generated [W]

References

1. Cronin, M.J. All-Electric vs. Conventional Aircraft: The Production/Operational Aspects. *J. Air.* **1983**, *20*, 481–486.
2. Sinnet, M. 787 No-Bleed Systems: Saving Fuel and Enhancing Operational Efficiencies. *Aero Q.* **2007**, *QTR_04|07*, 6–11.
3. Della Vecchia, P.; Stingo, L.; Nicolosi, F.; De Marco, A.; Cerino, G.; Ciampa, P.D.; Prakasha, P.S.; Fioriti, M.; Zhang, M.; Mirzoyan, A.; et al. Advanced turboprop multidisciplinary design and optimization within AGILE project. In Proceedings of the 2018 Aviation Technology, Integration, and Operations Conference, Atlanta, GA, USA, 25–29 June 2018; p. 3205.
4. Jones, R.I. The more electric aircraft—assessing the benefits. *J. Aero. Eng.* **2002**, *216*, 259–269.
5. Fioriti, M.; Vercella, V.; Viola, N. Cost-Estimating Model for Aircraft Maintenance. *AIAA J. Aircr.* **2018**, *55*, 1564–1575. https://doi.org/10.2514/1.C034664.
6. Chiesa, S.; Fioriti, M. UAV logistic support definition. In *Handbook of Unmanned Aerial Vehicles*; Springer: Dordrecht, The Netherlands, 2015; pp. 2565–2600. https://doi.org/10.1007/978-90-481-9707-1_79.
7. Raymer, D.P. *Aircraft Design: A Conceptual Approach*; AIAA Education Series: Washington, DC, USA, 1992.
8. Roskam, J. *Airplane Design*, 2nd ed.; Roskam Aviation and Engineering DAR Corporation Lawrence, KS, USA, 1989.
9. Torenbeek, E. *Synthesis of Subsonic Airplane Design*, 1st ed; Nijgh-Wolters-Noordhoff: Rotterdam, The Netherlands, 1976.
10. Martins Pires, R.M.; Lajux, V.; Fielding, J.P. Methodology for the Design and Evaluation of Wing Leading Edge and Trailing Edge Devices. In Proceedings of the International Congress of the Aeronautical Sciences, Hamburg, Germany, 3–8 September 2006.
11. Sobieszczanski-Sobieski, J. Multidisciplinary Design Optimization: An Emerging New Engineering Discipline. In *Advances in Structural Optimization*; Springer: Dordrecht, The Netherlands, 1995; pp. 483–496.
12. Werner-Westphal, C.; Heinze, W.; Horst, P. Multidisciplinary Integrated Preliminary Design Applied to Unconventional Aircraft Configuration. *J. Air.* **2008**, *45*, 581–590.
13. Allison, D.L.; Alyanak, E.J.; Shimmin, K. Aircraft system effects including propulsion and air cycle machine coupled interactions. In Proceedings of the 57th AIAA/ASCE/AHS/ASC Structures, Structural Dynamics, and Materials Conference, San Diego, CA, USA, 4–8 January 2016.
14. Jeyaraj, A.K.; Tabesh, N.; Liscouet-Hanke, S. Connecting Model-based Systems Engineering and Multidisciplinary Design Analysis and Optimization for Aircraft System Architecting. In Proceedings of the 2021 Aviation ForumVirtual Event, 2–6 August 2021.
15. Chakraborty, I.; Mavris, D.N. Integrated Assessment of Aircraft and Novel Subsystem Architectures in Early Design. In Proceedings of the 54th AIAA Aerospace Sciences Meeting, San Diego, CA, USA, 4–8 January 2016.
16. Ciampa, P.D.; Nagel, B.; La Rocca, G. A MBSE Approach to MDAO Systems for the Development of Complex Products. In Proceedings of the AIAA AVIATION 2020 FORUM, Virtual, 15–19 June 2020.
17. EASA. Certification Specifications for Normal, Utility, Aerobatic and Commuter Category Aeroplanes. *CS-23 Initial Issue* **2003**, *3*, 9.

18.　Fioriti, M.; Boggero, L.; Prakasha, P.; Mirzoyan, A.; Aigner, B.; Anisimov, K. Multidisciplinary aircraft integration within a collaborative and distributed design framework using the AGILE paradigm. *Pro. Aer. Sci.* **2020**, *119*, 100648.

19.　Woehler, S.; Atanasov, G.; Silberhorn, D.; Fröhler , B.; Zill, T. Preliminary Aircraft Design within a Multidisciplinary and Multifidelity Design Environment. In Proceedings of the Aerospace Europe Conference, Bordeaux, Frankreich, 25–28 February 2020.

20.　Liersch, C.; Hepperle, M.A. A distributed toolbox for multidisciplinary preliminary aircraft design. *CEAS Aer. J.* **2011**, *2*, 57–68.

21.　Zill, T.; Böhnke, D.; Nagel, B. Preliminary Aircraft Design in a Collaborative Multidisciplinary Design Environment. In Proceedings of the 11th AIAA Aviation Technology, Integration and Operations Conference. Virginia Beach, VA, USA, 20–22 September 2011.

22.　Torenbeek, E. *Synthesis of Subsonic Airplane Design*, 2nd ed.; Nijgh-Wolters-Noordhoff: Rotterdam, The Netherlands, 1984.

23.　Torenbeek, E. *Advanced Aircraft Design*, 1st ed.; Wiley Aerospace Series: Chichester, West Sussex, PO19 8SQ, United Kingdom, 2013.

24.　Jenkinson, L.R.; Simpkin, P.; Rhodes, D. *Civil Jet Aircraft Design*; Hodder Headline Group: London, UK, 1999.

25.　Wells, D.P.; Horvath, B.L.; McCullers, L.A. *The Flight Optimization System—Weights Estimation Method*; NASA Langley Research Center: Hampton, Virginia, USA, 2017.

26.　Chiesa, S.; Fioriti, M.; Viola, N. Methodology for an integrated definition of a System and its Subsystems: The case-study of an Airplane and its Subsystems. In*: Cogan, B. , editor. Systems Engineering - Practice and Theory [Internet]. London: IntechOpen; 2012. Available from: https://www.intechopen.com/chapters/32615 doi: 10.5772/34453*

27.　Nicolosi, F.; De Marco, A.; Attanasio, L.; Della Vecchia, P. Development of a Java-Based Framework for Aircraft Preliminary Design and Optimization. *J. Aerosp. Inf. Syst* **2016**, *13*, 234–242.

28.　De Marco, A.; Trifari, V.; Nicolosi, F.; Ruocco, M, A simulation-based performance analysis tool for aircraft design workflows. *Aerospace* **2020**, *7*, 155.

29.　Trifari, V.; Ruocco, M.; Cusati, V.; Nicolosi, F.; De Marco, A. Java Framework for Parametric Aircraft Design—Ground Performance. *Aircr. Eng. Aerosp. Technol.* **2017**, *89*, 599–608.

30.　Trifari, V. Development of a Multi-Disciplinary Analysis and Optimization framework and applications for innovative efficient regional aircraft. Ph.D. Thesis, University of Naples Federico II, 2020, Naples, Italy.